Distinct roles of septins in cytokinesis: SEPT9 mediates midbody abscission

Mathew P. Estey,[1,2] Caterina Di Ciano-Oliveira,[1] Carol D. Froese,[1] Margaret T. Bejide,[1,2] and William S. Trimble[1,2]

[1]Program in Cell Biology, Hospital for Sick Children, Toronto, Ontario M5G 1X8, Canada
[2]Department of Biochemistry, University of Toronto, Toronto, Ontario M5S 1A8, Canada

Septins are a family of GTP-binding proteins implicated in mammalian cell division. Most studies examining the role of septins in this process have treated the family as a whole, thus neglecting the possibility that individual members may have diverse functions. To address this, we individually depleted each septin family member expressed in HeLa cells by siRNA and assayed for defects in cell division by immunofluorescence and time-lapse microscopy. Depletion of SEPT2, SEPT7, and SEPT11 causes defects in the early stages of cytokinesis, ultimately resulting in binucleation. In sharp contrast, SEPT9 is dispensable for the early stages of cell division, but is critical for the final separation of daughter cells. Rescue experiments indicate that SEPT9 isoforms containing the N-terminal region are sufficient to drive cytokinesis. We demonstrate that SEPT9 mediates the localization of the vesicle-tethering exocyst complex to the midbody, providing mechanistic insight into the role of SEPT9 during abscission.

Introduction

Cell division is critical for the development of multicellular organisms. This process requires the proper coupling of chromosome segregation with the physical division of the cytoplasm (cytokinesis), which ensures that each daughter cell receives the correct complement of chromosomes and cellular material (Eggert et al., 2006). It has been demonstrated that cell division failure can cause genetic instability, ultimately leading to cancer (Fujiwara et al., 2005). In mammals, cell division involves the constriction of a contractile ring, which pinches the mother cell into two daughter cells once chromosome segregation has occurred (Glotzer, 2001). The final separation of daughter cells occurs via a process referred to as abscission, in which an intercellular microtubule bridge called the midbody is severed.

Septins are a family of highly conserved proteins, of which there are 14 members in humans (SEPT1–SEPT14; Weirich et al., 2008). They consist of a central conserved GTP-binding domain flanked by N- and C-terminal extensions of varying length and divergent sequence. Many septin family members undergo complex alternative splicing, making the number of unique septin polypeptides even greater (Hall and Russell, 2004). These proteins associate with each other to form ordered oligomeric complexes and filaments (Sirajuddin et al., 2007), which are thought to regulate a vast array of cellular processes, including membrane traffic (Beites et al., 1999), phagocytosis (Huang et al., 2008), spermatogenesis (Ihara et al., 2005; Kissel et al., 2005), and dendrite branching (Tada et al., 2007; Xie et al., 2007).

Septins are also important for cell division in many different organisms (Hall et al., 2008b). Work in mammalian cells showed that injection of SEPT2 antibodies at anaphase/telophase impaired the completion of cytokinesis (Kinoshita et al., 1997). Simultaneous depletion of SEPT2, SEPT6, and SEPT7 (and possibly others) from HeLa cells resulted in accumulation of cells with multiple or fragmented nuclei (Kremer et al., 2005; Spiliotis et al., 2005). These studies took advantage of the observation that depletion of one septin can result in the depletion of other septin family members, a phenomenon that is thought to result from destabilizing the septin complex (Kinoshita et al., 2002). Finally, SEPT9 depletion from HMEC and HeLa cells caused cytokinetic defects (Surka et al., 2002; Nagata et al., 2003), although it was not clear whether the expression of other septins was affected.

M.P. Estey and C. Di Ciano-Oliveira contributed equally to this paper.
Correspondence to William S. Trimble: wtrimble@sickkids.ca
Abbreviations used in this paper: KD, knockdown; mAb, monoclonal antibody.

The Rockefeller University Press $30.00
J. Cell Biol. Vol. 191 No. 4 741–749
www.jcb.org/cgi/doi/10.1083/jcb.201006031

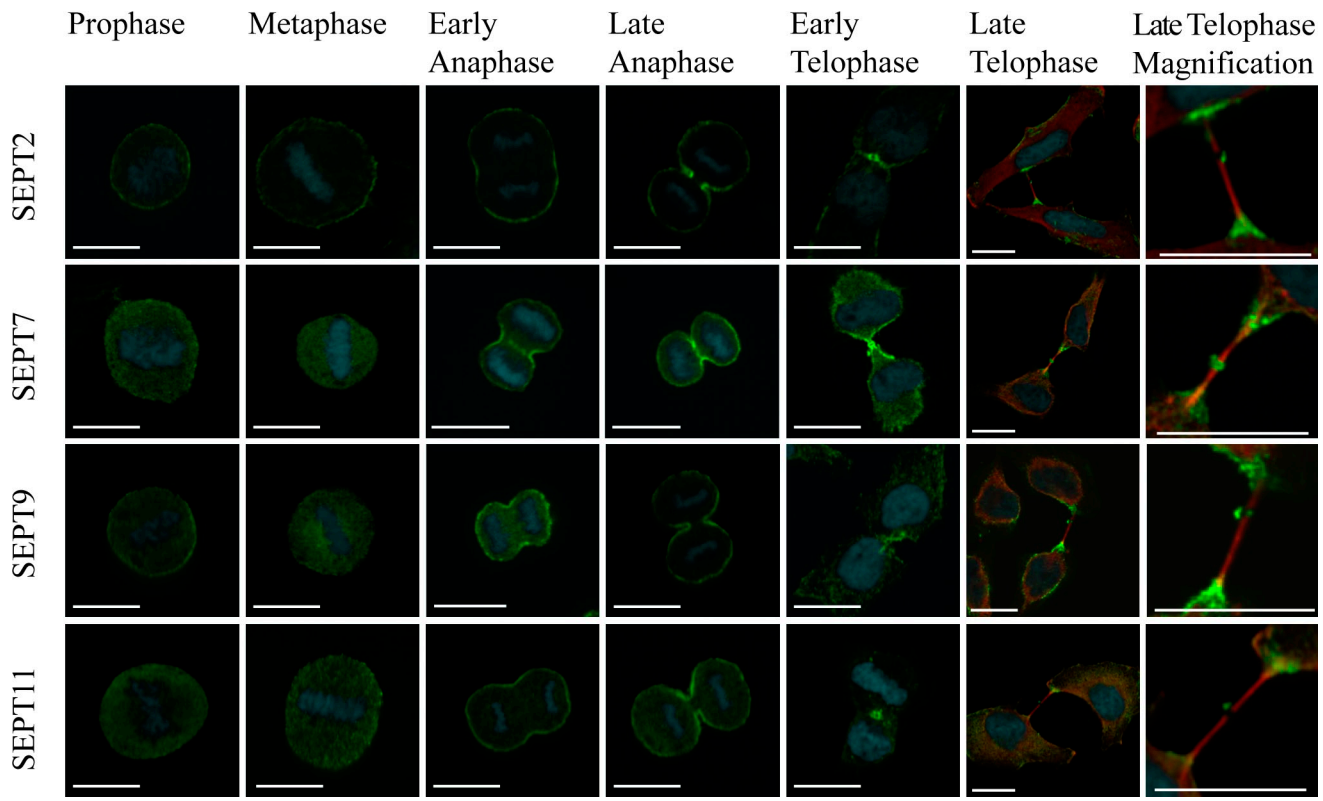

Figure 1. **Septin distribution during cell division.** HeLa cells were stained for α-tubulin (red), DNA (blue), and the indicated septin (green). Confocal microscopy was performed, and a single z slice is shown. Bars, 17 µm.

Recent work demonstrated that SEPT2 acts as a scaffold for myosin II and its kinases at the cleavage furrow, thus facilitating the full activation of myosin II that is required for cleavage furrow stability (Joo et al., 2007). SEPT7 has been shown to mediate the localization of CENP-E to kinetochores, which is important for proper chromosome segregation (Zhu et al., 2008). However, it is unclear whether other septin family members within the septin complex are also important for these processes. Consequently, although it is well established that the septin family is important for mammalian cell division, it remains elusive whether these proteins act together to perform the same role, or whether they have different functions during cell division.

Results and discussion

To examine the role of individual septins in cell division, we first determined the expression profile of septins in HeLa cells. Western blotting with our septin antibodies (which may not recognize all isoforms) showed that HeLa cells contain SEPT2, SEPT6, SEPT7, SEPT9, and SEPT11 (Fig. S1 A). We next assessed the distribution of these septins during cell division (Fig. 1). In prophase and metaphase, SEPT2 showed cortical enrichment, whereas the others had a more diffuse cytosolic distribution. All septins accumulated at the cleavage furrow during anaphase, and appeared at both sides of the intercellular bridge and the midbody in telophase. Although our SEPT6 antibody had high background staining, it showed a similar distribution to SEPT11 (unpublished data). Occasionally, septins were visualized on spindle microtubules as reported by others (Spiliotis et al., 2005). Double labeling showed that SEPT9 colocalizes with each other septin during anaphase and telophase (Fig. S1, B–E). In addition, immunoprecipitation analysis suggested that septin complex composition is largely unaltered upon mitotic entry (Fig. S1, F and G). Likewise, no obvious differences in septin complex composition were observed when immunoprecipitations were performed from cells enriched at the later stages of cell division (Fig. S1, H and I). However, we cannot rule out the possibility that subtle rearrangements of septin subunits or septin polymerization state occur during cell division.

Next, we selectively depleted each septin expressed in HeLa cells by siRNA (Fig. 2 A) and assayed for cytokinesis defects. SEPT6 knockdown (KD) had no adverse effects (Fig. 2 C), although this could reflect incomplete silencing. Depletion of SEPT2 and SEPT11 increased the number of multinucleated cells to 11% and 15%, respectively, compared with 3% of cells transfected with control siRNA (Fig. 2 C). Treatment with SEPT7 siRNA depleted all septins, as described previously (Kinoshita et al., 2002; Kremer et al., 2005; Tooley et al., 2009), and increased the number of multinucleated cells to 26% (Fig. 2 C). Although SEPT9 KD also resulted in an increase in multinucleated cells (8%), we observed a second, more prominent cytokinetic defect (Fig. 2, B and C). Strikingly, 23% of SEPT9 KD cells remained joined by a microtubule bridge (midbody), compared with 6% of cells transfected with control siRNA. Expression of siRNA-resistant SEPT9 rescued these cytokinetic defects (see Fig. 4), which demonstrates that this phenotype is

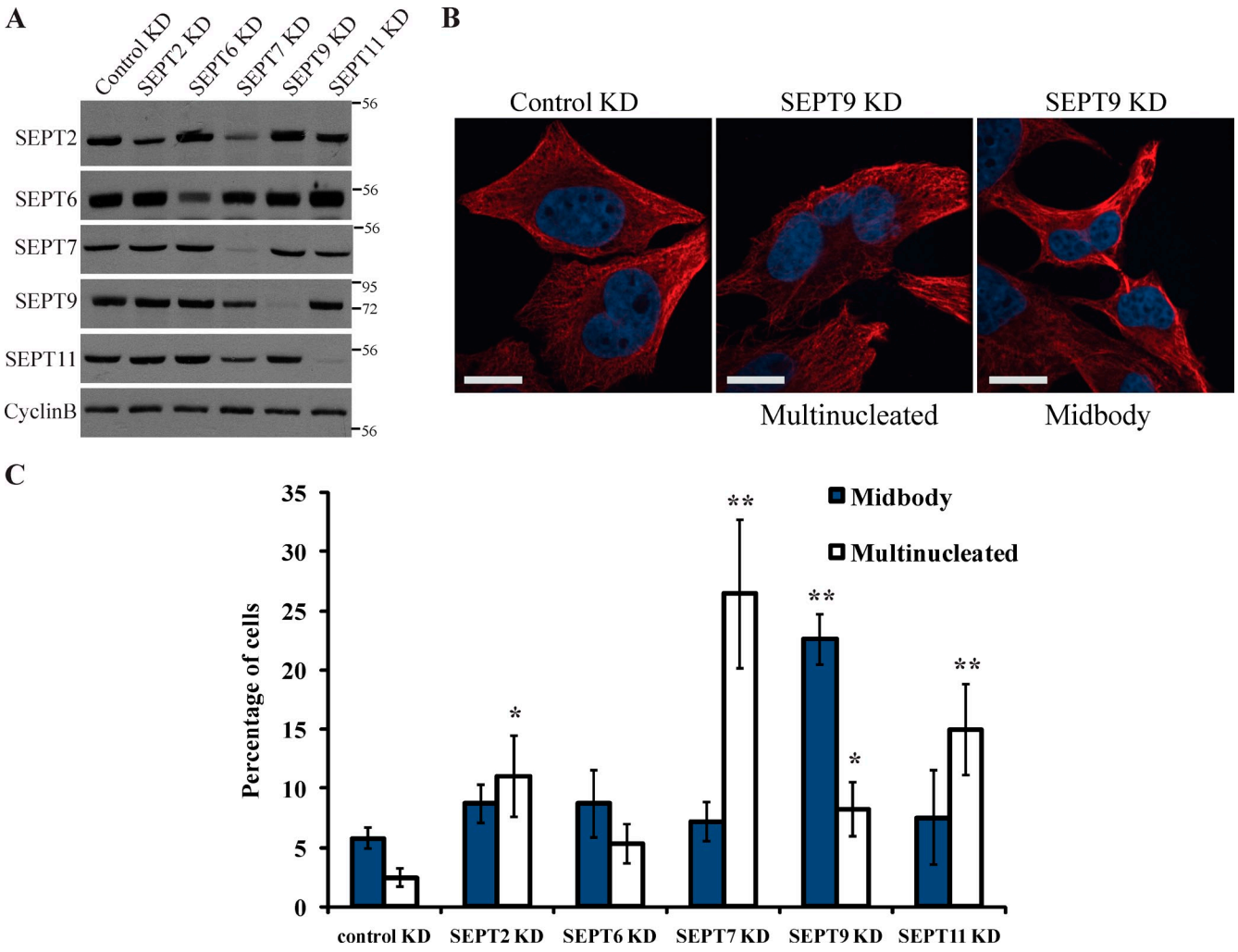

Figure 2. **Roles of individual septins in cell division.** (A) HeLa cells were treated with the indicated siRNA, and lysates were probed as specified. Numbers to the right of the blot represent molecular mass standards in kilodaltons. (B) Representative examples of cells treated with control siRNA, and of multinucleated cells and cells attached by persistent midbodies after SEPT9 KD (red, α-tubulin; blue, DNA). Bars, 17 µm. (C) Quantification of effect of septin KD on cytokinesis. The percentage of cells exhibiting multinucleation or midbody attachment was determined upon treatment with the indicated siRNA. Data are represented as mean ± SEM (error bars; $n \geq 300$ cells from three or more independent experiments). Asterisks indicate differences between control and septin KD cells. *, $P < 0.01$; **, $P < 0.0001$.

specifically caused by depletion of SEPT9 and is not the result of off-target effects of our siRNA. Similar defects were observed upon SEPT9 KD in HEK293 cells (Fig. S1, J and K), arguing that this is not a HeLa cell–specific phenomenon. Intriguingly, this late telophase arrest was not observed upon depletion of any other septin (Fig. 2 C). Our results suggest that although septins coexist in complexes, they may have distinct functions during cell division.

To address this, we followed septin-depleted cells through cell division by time-lapse microscopy. Separation of the DNA, ingression of the cleavage furrow, and formation of the midbody appeared normal upon control KD (Fig. 3 A and Video 1). However, SEPT2 (Video 2)- and SEPT11 (Fig. 3 B and Video 3)-depleted cells exhibited abnormal cleavage furrow contraction at the early stages of cytokinesis. Although cleavage furrow ingression began normally, the size of the nascent daughter cells then fluctuated dramatically. In most cases, the cleavage furrow did eventually fully ingress; however, it did so to the side of both daughter nuclei, thus generating a multinucleated cell and an enucleated cell. In a few cases, cleavage furrow regression was observed, as described previously (Spiliotis et al., 2005). Depletion of all septins with SEPT7 siRNA had the same effects. A similar phenotype has been observed upon depletion of the septin-binding protein anillin (Straight et al., 2005), raising the possibility that SEPT2 and SEPT11 may mediate anillin function during cytokinesis.

Despite the increase in multinucleated cells observed upon SEPT9 KD (Fig. 2 C), these cells showed no defects in DNA separation, cleavage furrow constriction, or midbody formation (Fig. 3 C and Video 4). Instead, SEPT9-depleted cells exhibited dramatic defects in midbody abscission (Fig. 3 C and Video 5). The midbody of control KD cells abscised an average of 3.9 h after the onset of cytokinesis, and all of these cells successfully completed abscission (Fig. 3 D). In contrast, only 70% of SEPT9 KD cells successfully abscised, with the mean abscission time being 9 h after the initiation of cytokinesis (Fig. 3 D;

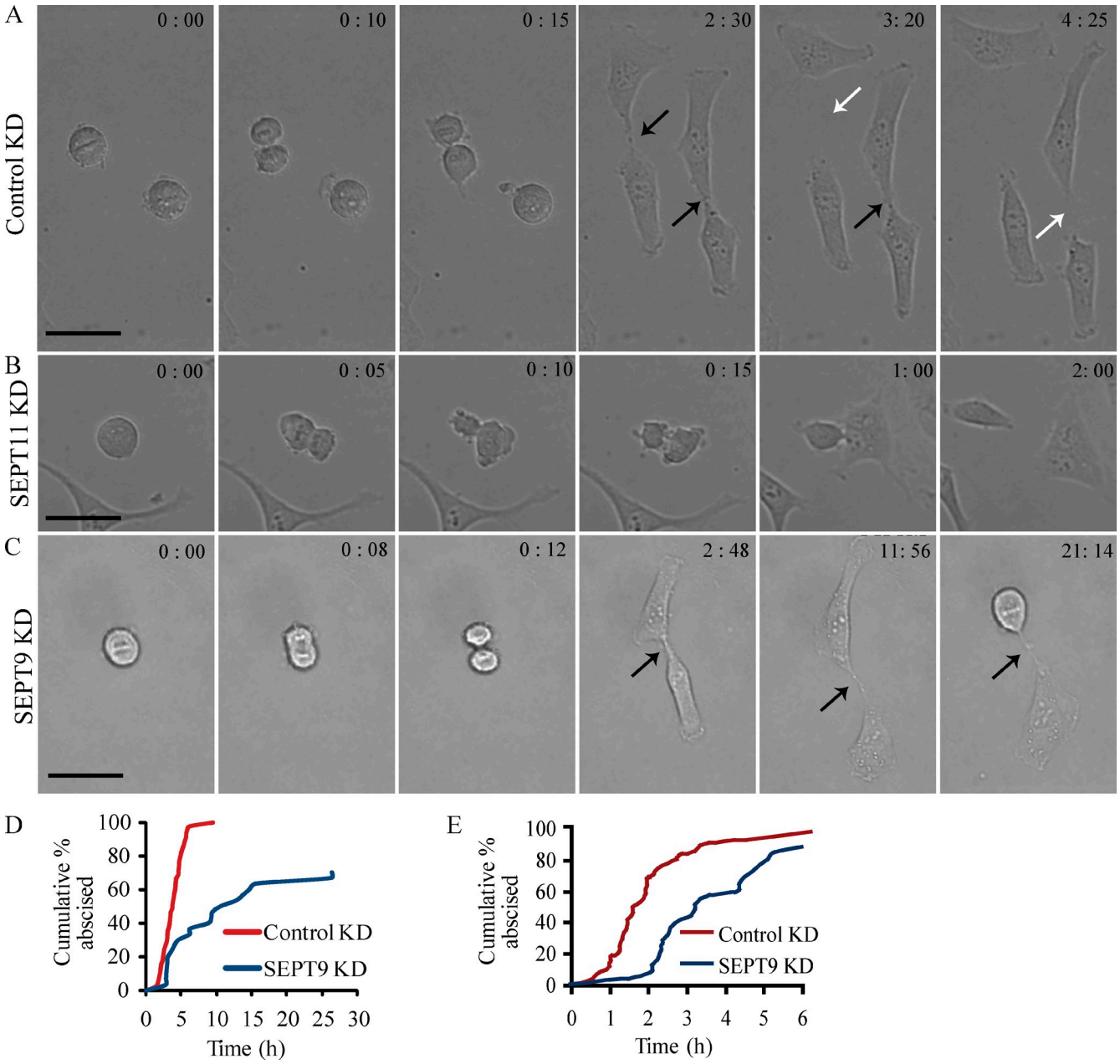

Figure 3. **SEPT9 mediates midbody abscission.** (A–C) HeLa cells were transfected with siRNA, and randomly selected cells were followed through division by time-lapse microscopy. The time (in hours:minutes) since the beginning of DNA segregation is shown. Black arrows point to intact midbodies, whereas white arrows denote abscission. Bars, 32 µm. (A) Division of HeLa cells after treatment with control siRNA. (B) SEPT11 KD causes defects early in cytokinesis. (C) SEPT9 KD causes defects in midbody abscission. See Videos 1–5 for complete movies. (D and E) Quantification of the effect of SEPT9 KD on midbody abscission in HeLa (D) and ARPE-19 cells (E). The time from DNA segregation to midbody abscission was determined, and the cumulative percentage of cells that were abscised is plotted as a function of time. For D, $n = 45$ cells for control KD and $n = 30$ cells for SEPT9 KD; for E, $n = 34$ cells for control KD and $n = 25$ cells for SEPT9 KD.

$P < 0.0001$). Remarkably, in 20% of SEPT9 KD cells, the midbody either persisted until the next division (Fig. 3, C and D) or had not broken 40 h after the onset of cytokinesis. In some cases, the midbody broke when both daughter cells reentered mitosis, whereas in other cases it persisted even after a second round of division. The remaining 10% of SEPT9 KD cells exhibited one of two phenotypes: either the midbody regressed after failing to abscise, giving rise to a multinucleated cell (thus accounting for our fixed-cell results), or one or both daughter cells underwent apoptosis after being unable to complete abscission. Impaired midbody abscission upon SEPT9 KD was also observed in noncancerous human retinal pigment epithelial cells (ARPE-19), which have normal karyology (Figs. 3 E and S1 L; Dunn et al., 1996). In these cells, SEPT9 KD increased the mean abscission time to 4.2 h, compared with 2.3 h for cells transfected with control siRNA ($P < 0.01$). These cells are highly motile, and may therefore complete abscission by mechanical rupture of the midbody (Steigemann and Gerlich, 2009), which might possibly explain the faster abscission time and less-penetrant SEPT9 KD phenotype. Collectively, our

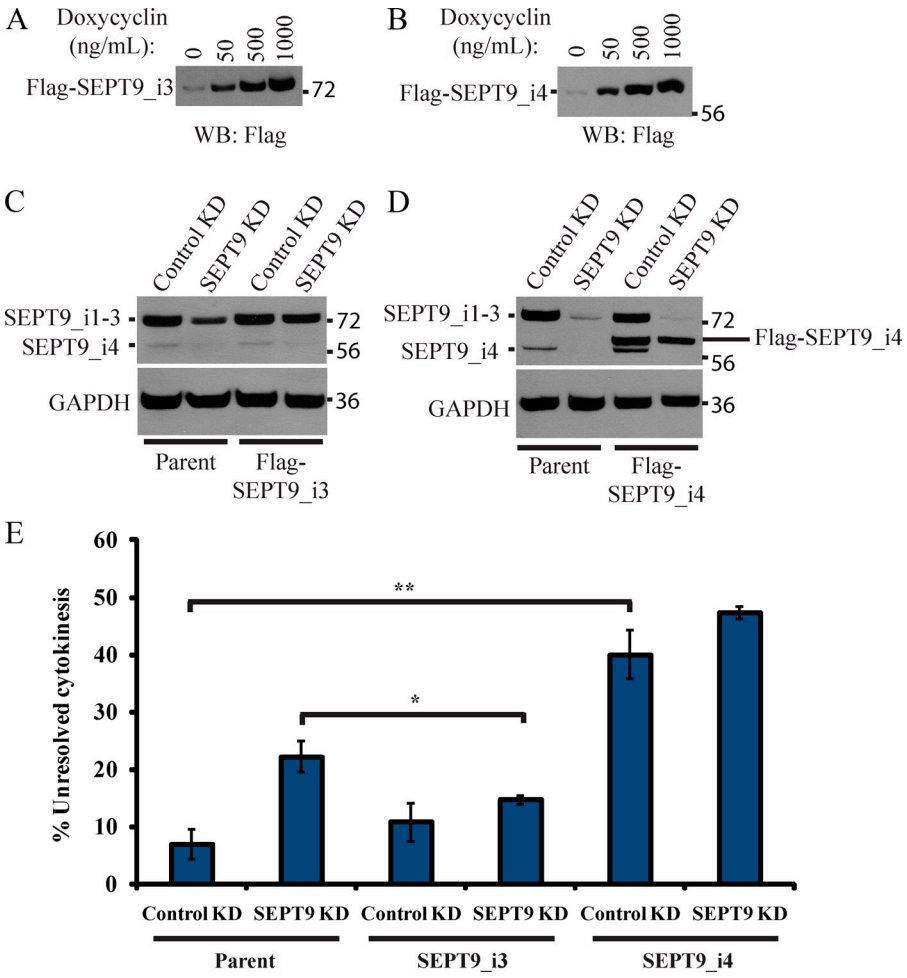

Figure 4. **The SEPT9 isoforms are not all functionally equivalent.** (A and B) Stable cell lines inducibly expressing siRNA-resistant Flag-SEPT9_i3 (A) or Flag-SEPT9_i4 (B) were treated with increasing amounts of doxycycline, and expression was assayed by Western blotting. (C) The parent and Flag-SEPT9_i3 cell lines were treated with control or SEPT9 siRNA in the absence of doxycycline, and SEPT9 levels were assayed by Western blotting. Note that SEPT9_i4 disappears upon treatment with SEPT9 siRNA, demonstrating efficient KD. Also note the higher SEPT9 (_i1-3) levels in the Flag-SEPT9_i3 stable line upon SEPT9 depletion, when compared with the parent line. (D) The parent and Flag-SEPT9_i4 cell lines were treated as in C. Numbers to the right of the blots represent molecular mass standards in kilodaltons. (E) The parent, Flag-SEPT9_i3, and Flag-SEPT9_i4 cell lines were treated with control or SEPT9 siRNA and assayed for defects in cytokinesis by immunofluorescence microscopy. Unresolved cytokinesis refers to cells exhibiting midbody attachment or multinucleation. Data are represented as mean ± SEM (error bars; $n \geq 300$ cells from three or more independent experiments). *, $P < 0.05$; **, $P < 0.005$.

results suggest that septins contribute distinct functions at different stages of cell division: SEPT9 is important for mediating midbody abscission at the terminal stage of cytokinesis, whereas SEPT2 and SEPT11 have roles earlier in cytokinesis. It remains unclear whether other septins are also involved in abscission, as such a role may be obscured by the early cytokinesis defects that occur upon their depletion.

Given the unique phenotype observed upon specific depletion of SEPT9, we decided to focus our attention on the role of SEPT9 during cell division. Because of complex alternative splicing, there are five N-terminal variants of SEPT9 (Fig. S2 A). These are referred to as isoforms 1–5 (_i1 to _i5; Hall et al., 2008a), and HeLa cells express all isoforms except _i2 (Burrows et al., 2003). Because our SEPT9 siRNA targets all isoforms, we assessed whether individual isoforms are capable of rescuing the cytokinetic defect observed upon SEPT9 depletion. To this end, we generated a stable cell line that expresses siRNA-resistant SEPT9_i3 under the control of an inducible promoter (Fig. 4 A). In the absence of induction, this cell line exhibits low levels of leaky expression comparable to endogenous SEPT9 levels. First, we verified that SEPT9 KD in the parent cell line, from which the SEPT9_i3 stable line was derived, caused the expected cytokinetic defects (persistent midbodies and multinucleation resulting from abscission failure, which we refer to collectively as "unresolved cytokinesis"; Fig. 4, C and E). In contrast, the basal expression of siRNA-resistant SEPT9_i3 significantly reduced these defects (Fig. 4, C and E; compare SEPT9 KD in the parent cell line to SEPT9 KD in the SEPT9_i3 cell line). This not only demonstrates the specificity of our SEPT9 siRNA, but also argues that SEPT9_i3 is sufficient to drive cytokinesis in the absence of the other SEPT9 isoforms. Similar results were obtained with SEPT9_i1 (unpublished data), which only differs from SEPT9_i3 at the extreme N terminus (Fig. S2 A). SEPT9_i2 was not tested because it is not expressed in HeLa cells (Burrows et al., 2003).

SEPT9_i4 lacks the SEPT9 N-terminal region (Fig. S2 A), and has been shown to be overexpressed in many tumors (Burrows et al., 2003; Scott et al., 2006). To assess whether SEPT9_i4 is also sufficient to drive cytokinesis in the absence of other SEPT9 isoforms, we generated a stable cell line that inducibly expresses siRNA-resistant SEPT9_i4 (Fig. 4 B). The basal expression of SEPT9_i4 in this cell line is similar to the expression level of endogenous SEPT9_i1–_i3 (Fig. 4 D). Interestingly, this level of SEPT9_i4 expression in itself induced persistent midbodies and multinucleation (Figs. 4 E and S2 B; compare control KD in the parent cell line to control KD in the SEPT9_i4 cell line). These defects were not suppressed by depleting endogenous SEPT9 (Figs. 4 E and S2B), which suggests that they are not simply the result of increased total SEPT9 levels. Further, depletion of endogenous SEPT9 in the SEPT9_i4 cell line did not cause an increase in cytokinesis

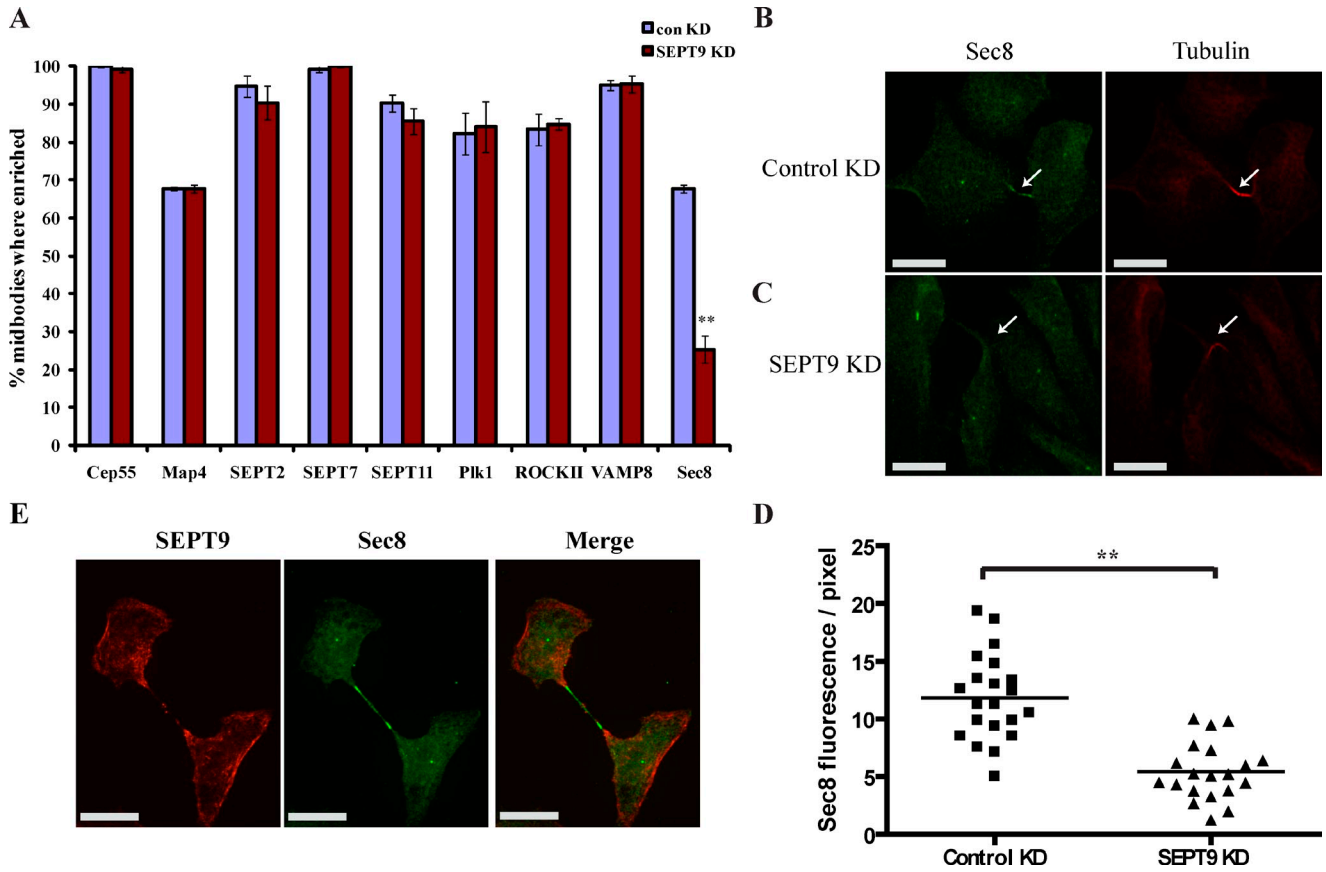

Figure 5. **SEPT9 mediates exocyst complex localization to the midbody.** (A) Quantification of the effect of SEPT9 KD on the localization of midbody components. The percentage of cells exhibiting enrichment of the protein of interest at the midbody was determined by immunofluorescence microscopy after control or SEPT9 KD. Data are represented as mean ± SEM (error bars; $n \geq 300$ cells from three independent experiments). Asterisks indicate differences between control and SEPT9 KD cells; **, $P < 0.001$. (B and C) Representative example of the localization of the exocyst component Sec8 in cytokinetic cells upon control (B) or SEPT9 KD (C). Arrows point to the midbody. (D) Sec8 fluorescence at the midbody was quantified using ImageJ upon control or SEPT9 KD; **, $P < 0.0001$. (E) Double staining of SEPT9 and Sec8 in cytokinetic cells. Bars, 17 µm.

defects, which indicates that SEPT9_i4 is acting in a dominant-negative fashion. In contrast, inducing SEPT9_i3 expression up to 330% of total endogenous SEPT9 did not cause cytokinetic defects (unpublished data). SEPT9_i5 was not tested, as it is not recognized by our SEPT9 antibody. Our data point to an important role for the N-terminal region of SEPT9 in cytokinesis, which will be the subject of future study. Intriguingly, this region contains several putative phosphorylation sites, which could be important for SEPT9 function. These results suggest that even individual isoforms of a given septin can have diverse functions.

We next wanted to elucidate the molecular mechanism by which SEPT9 mediates abscission. We hypothesized that SEPT9 may help localize specific factors that are important for abscission at the midbody. To address this, we examined the localization of several midbody components upon SEPT9 depletion. These included: SEPT2, SEPT7, and SEPT11; Cep55, a microtubule-bundling protein important for midbody integrity (Zhao et al., 2006); MAP4, a microtubule-stabilizing protein that associates with some septins (Kremer et al., 2005); Plk1, a regulator of cytokinesis (Petronczki et al., 2007); ROCKII, a kinase important for the completion of cytokinesis (Lowery et al., 2007); VAMP8, a SNARE protein that is thought to mediate vesicle fusion at the midbody (Gromley et al., 2005; Low et al., 2003); and Sec8, a component of the exocyst complex that mediates vesicle tethering at the midbody (Gromley et al., 2005). SEPT9 KD had no effect on the midbody localization of other septins, Cep55, MAP4, Plk1, ROCKII, or VAMP8 (Fig. 5 A and Fig. S3). In contrast, depletion of SEPT9 resulted in a drastic loss of the exocyst component Sec8 at the midbody (Fig. 5). In control KD cells, Sec8 was enriched at 68% of midbodies; however, only 25% of SEPT9 KD cells exhibited Sec8 enrichment at the midbody (Fig. 5, A–C). Quantification of Sec8 fluorescence at the midbody verified these observations (Fig. 5 D). Previous work suggests that exocyst-dependent tethering of vesicles at the midbody facilitates their fusion with the plasma membrane and with each other, thus contributing to abscission (Gromley et al., 2005). Depletion of exocyst subunits results in abscission defects remarkably similar to those observed upon SEPT9 depletion (Gromley et al., 2005). SEPT9 is not important for the localization of most of the midbody proteins tested, but plays an important role in mediating exocyst complex localization to the midbody, where it facilitates vesicle fusion that is important for abscission. Interestingly, SEPT9 and Sec8 did not colocalize at the midbody, but were found directly adjacent to each other (Fig. 5 E). Similar results have been observed in yeast, where septins act to

compartmentalize the exocyst at the site of cleavage (Dobbelaere and Barral, 2004). Although more work is required to elucidate how SEPT9 regulates exocyst localization, this study has provided significant insight into the molecular function of SEPT9 during cell division.

We have demonstrated that specific depletion of SEPT9 in HeLa, HEK293, and ARPE-19 cells causes defects in midbody abscission. Although deletion of the *Sept9* gene in mice is embryonic lethal, embryos survive for 10 d before expiring, arguing that successful cell division can occur in the absence of SEPT9 (Kinoshita, 2008). A possible explanation for this apparent discrepancy is that abscission is not an absolute requirement for subsequent rounds of cell division. Consistent with this, SEPT9 KD or expression of SEPT9_i4 resulted in some cells that were connected by persistent midbodies to multiple other cells. Similar results have been observed upon depletion of exocyst subunits (Gromley et al., 2005). In fact, *Sec8* knockout embryos display no obvious phenotype up to embryonic day 6.5 (Friedrich et al., 1997). Further, during embryonic development, blastomeres often remain joined by intercellular bridges for several rounds of division (Goodall and Johnson, 1984; Eggert et al., 2006). Finally, the SEPT9 KD phenotype is incompletely penetrant so that some cells still do eventually divide normally, whereas others apparently achieve midbody breakage by mechanical strain caused by the subsequent division of the daughter cells. These observations could also contribute to the survival of SEPT9 knockout embryos.

A significant body of work has linked alterations in SEPT9 expression to cancer (Scott et al., 2005). Some of these instances involve a loss of SEPT9 function (Osaka et al., 1999; Russell et al., 2000; Yamamoto et al., 2002), whereas others involve SEPT9 overexpression, either through amplification of the *SEPT9* gene (Montagna et al., 2003) or increased expression of SEPT9_i4 (Burrows et al., 2003; Scott et al., 2006) or SEPT9_i1 (Scott et al., 2006; Gonzalez et al., 2007). The results presented here suggest that loss of SEPT9 function impairs the completion of cell division. This may result in genomic instability, ultimately contributing to cancer (Fujiwara et al., 2005). Increased expression of SEPT9_i4 could have similar consequences, as we have demonstrated that modest increases in SEPT9_i4 levels cause defects in cytokinesis.

By specifically depleting SEPT9, we were able to elucidate the fact that this protein plays an important role in midbody abscission, a phenotype that is masked by simultaneous depletion of other septins. Therefore, although depletion of all septin family members provides a good starting point for probing septin function, it will be important to analyze the role of individual septins in septin-dependent processes. Our work further suggests that a complete understanding of septin function will also require careful consideration of the function of individual septin isoforms.

Materials and methods

Cell culture

HeLa, HEK293, and ARPE-19 cells were obtained from the American Type Culture Collection. HeLa and HEK293 cells were cultured as described previously (Surka et al., 2002), and ARPE-19 cells were grown in DME/F-12 (Lonza) with 10% FBS.

Western blotting

Western blotting was performed according to standard procedures using the following primary antibodies: SEPT9 (Surka et al., 2002), SEPT11 (Huang et al., 2008), SEPT2 (Xie et al., 1999), SEPT6 (Huang et al., 2008), SEPT7 (a gift from B. Zieger, University Hospital Freiberg, Freiberg, Germany), GAPDH (Millipore), Flag (Sigma-Aldrich), and CyclinB (Santa Cruz Biotechnology, Inc.).

siRNA treatment

siRNA for SEPT2 (5′-GAATATTGTGCCTGTCATTG-3′), SEPT6 (5′-CCTGAAGTCTCTGGACCTAGT-3′), SEPT7 (5′-TATATGCTGCACTGAATGGAA-3′), SEPT9 (5′-GCACGATATTGAGGAGAAA-3′), SEPT11 (5′-CAAGAGGAATTGAAGATTAAA-3′), and control siRNA (5′-GCAGCGACCATGAGTATCA-3′) were obtained from Thermo Fisher Scientific. Cells grown to 60–80% confluence in 6-well plates were transfected with 120–240 pmol of double-stranded siRNA using Lipofectamine 2000 (Invitrogen). KD was achieved after 56–72 h. For siRNA treatment of stable cells lines, antibiotics were removed before transfection.

Immunofluorescence microscopy

Immunofluorescence microscopy was performed as described previously (Di Ciano-Oliveira et al., 2005) for analysis of cytokinetic defects (Figs. 2 and 4). Any cells connected via a microtubule bridge, as judged by α-tubulin staining (Sigma-Aldrich), were counted as being connected by a midbody. Any cell having more than one nucleus, as judged by Hoescht staining, was counted as being multinucleated. For analysis of the localization of septins and midbody components (Figs. 1, 5, S1 C–E, and S3), cells were fixed for 5 min at 37°C with 2% paraformaldehyde in PBS, inactivated for 15 min at 37°C with 25 mM glycine and 25 mM ammonium chloride in PBS, permeabilized for 15 min at room temperature with 0.2% Triton X-100 in PBS, and blocked for 1 h in PBS with 0.1% saponin, 1% horse serum, and 2% BSA. Cells were then incubated with the following primary antibodies: Sec8 (Abcam), Map4 (BD), Plk1 (Invitrogen), SEPT2 (Xie et al., 1999), SEPT7 (Santa Cruz Biotechnology, Inc.), SEPT9 (Surka et al., 2002), SEPT11 (Huang et al., 2008), VAMP8 (a gift from T. Weimbs, University of California, Santa Barbara, Goleta, CA), and α-tubulin (Sigma-Aldrich) or α/β-tubulin (Cell Signaling Technology). For Cep55, cells were transfected with GFP-*Cep55* (a gift from K. Kutsche, Universitätsklinikum Hamburg-Eppendorf, Hamburg, Germany) 2 d after treatment with control or SEPT9 siRNA. For ROCKII, cells were fixed with methanol, blocked in PBS with 10% FBS, and incubated with ROCKII antibody (Millipore). Cells were imaged using an inverted fluorescence microscope (DMIRE2; Leica) equipped with a back-thinned EM charge-coupled device camera (Hamamatsu) and spinning disk confocal scan head. The unit was equipped with four separate diode-pumped solid-state laser lines (405 nm, 491 nm, 561 nm, and 638 nm; Spectral Applied Research), a motorized xy stage (ASI), an Improvision Piezo Focus Drive (PerkinElmer), and a 1.5× magnification lens (Spectral Applied Research). The equipment was driven by Volocity acquisition software, and powered by a Power Mac G5 (Apple).

Time-lapse microscopy

HeLa and ARPE-19 cells treated with the indicated siRNA were imaged in HPMI (RPMI powder [Invitrogen] supplemented with 15 mM sodium chloride and 20 mM Hepes, pH 7.4) at 37°C on an inverted microscope (TE2000; Nikon) adapted with a Solent environmental chamber. A Nikon Plan-Fluor 40×/0.6 NA objective was used in combination with a charge-coupled device camera (Orca AG; Hamamatsu). The Improvision Volocity 4.2 software suite was used for image acquisition, analysis, and manipulation. The time from the beginning of chromosome segregation to midbody abscission was determined for each cell that started division within the first 24 h of imaging. Cells that were multinucleated before division were excluded from analysis.

Generation and characterization of stable cell lines

Stable cell lines were generated using the Retro-X Tet-On Advanced Inducible Expression System (Takara Bio Inc.). pRetroX-Tet-On-Advanced was transfected into FLYRD18 packaging cells (a gift from C. Tailor and S. Duffy, Hospital for Sick Children, Toronto, Canada) using the calcium phosphate method, and the media was changed 24 h later. After an additional 24 h, the virus-containing media was filtered (using a 0.2 µm HT Tuffryn filter; Pall), and polybrene (Sigma-Aldrich) was added to 8 µg/ml. The virus-containing media was then added to wild-type HeLa cells, and the media was subsequently changed 4–6 h after infection. 2 d later, G418 was added to a final concentration of 500 µg/ml. Individual colonies were expanded and

screened for the presence of the Tet-Advanced transactivator by Western blotting with the TetR antibody (Takara Bio Inc.). This yielded the parent HeLa Tet-On cell line. Transcripts encoding SEPT9_i3 and SEPT9_i4 (a gift from E. Petty, University of Michigan, Ann Arbor, MI) were Flag-tagged and made siRNA-resistant by introducing three silent point mutations into the siRNA target sequence, then subsequently cloned into pRetroX Tight Pur (Takara Bio Inc.). These plasmids were then individually transfected into FLYRD18 packaging cells, and the resulting viruses were used to infect the parent HeLa Tet-On cell line (which was maintained in 250 µg/ml G418). 2 d after virus infection, puromycin was added to a final concentration of 1 µg/ml. Individual colonies were expanded and screened for the presence Flag-SEPT9_i3 or Flag-SEPT9_i4 by induction with various amounts of doxycycline and Western blotting with anti-Flag (Sigma-Aldrich) or anti-SEPT9 antibodies. The resulting cell lines, which inducibly express siRNA-resistant SEPT9_i3 or SEPT9_i4, were maintained in DME with 10% FBS, 1% antibiotics, 500 µg/ml G418, and 1 µg/ml puromycin.

Generation and testing of the SEPT9 monoclonal antibody (mAb 10C10)

Human septins 1, 2, 5, 6_i2, 7, 8, 9_i1, 11, and 12_i2 were cloned into pFastBacHTa (Invitrogen) using the 5′ EcoRI and 3′ XhoI sites. Silent mutations were first introduced into any internal EcoRI or XhoI sites in the septins. Baculoviruses were prepared according to manufacturer's instructions and used to infect 50 mL of suspended SF21 cells for 144 h. These cells were pelleted and resuspended in lysis buffer (50 mM Hepes, pH 7.5, 200 mM magnesium sulfate, 200 mM ammonium sulfate, 150 mM sucrose [Low and Macara, 2006], and 25 mM imidazole). Immediately before French pressing, protease inhibitors were added. The lysates were centrifuged at 20,000 *g* for 20 min, and the supernatants were incubated with 250 µl of nickel-nitrilotriacetic acid agarose (QIAGEN) for 1 h, rotating end over end. The beads were pelleted and washed three times in lysis buffer before being transferred to a column, and the proteins were eluted with lysis buffer containing 500 mM imidazole. The proteins were quantified using protein reagent (Bio-Rad Laboratories) and examined for purity by SDS-PAGE and Coomassie staining. Monoclonal antibodies were prepared by the Monoclonal Antibody Facility at the Hospital for Sick Children, using 5 mL of a 0.5 mg/ml septin mixture containing human septins 1, 2, 5, 6_i2, 7, 8, 9_i1, 11, and 12_i2. 16 hybridomas recognizing the antigens were screened for reactivity with individual septins, the His-S tag present on each of the septins, and SF21 cell lysate. One hybridoma (10C10) produced antibody specific to SEPT9. For Western blotting, ∼10 ng of each recombinant septin was analyzed using 10C10 at 1:500.

Immunoprecipitation

Cells were arrested in mitosis by adding nocodazole (Sigma-Aldrich) to the culture medium to a final concentration of 50 ng/ml, then incubated for ∼16 h. To enrich for the later stages of cell division, nocodazole-arrested cells were plated on poly-D-lysine–coated dishes, washed extensively after attachment, and lysed at the indicated time after release. Cells were lysed in Triton X-100 lysis buffer (30 mM Hepes, pH 7.5, 100 mM sodium chloride, 1 mM EGTA, 1% Triton X-100, and 20 mM sodium fluoride) with additional phosphatase (1 mM sodium orthovanadate, 100 nM okadaic acid, and 100 nM calyculin A) and protease inhibitors. Approximately 1 µg of antibody was added to ∼1 mg of lysate and incubated at 4°C with constant mixing for at least 1 h. After washing with Triton X-100 lysis buffer, 30 µl of protein A–Sepharose (Sigma-Aldrich) was added to the antibody–lysate mixture, and incubated at 4°C with constant mixing for at least 1 h. The beads were then washed three times, resuspended in SDS-PAGE loading buffer containing n-ethyl-maleimide, and subjected to Western blotting.

Statistical analysis

Two-tailed Student's *t* tests were applied to determine statistical significance.

Online supplemental material

Fig. S1 shows the expression profile of septins in HeLa cells, and a characterization of our SEPT9 mAb. It also shows that septin complex composition is largely unaltered upon mitotic entry and throughout cell division, and that SEPT9 depletion in HEK293 cells causes persistent midbodies and multinucleation. The extent of SEPT9 depletion in ARPE-19 cells is also shown. Fig. S2 contains an alignment of the SEPT9 isoforms, and shows that SEPT9_i4 expression induces both persistent midbodies and multinucleation. Fig. S3 shows that the localization of Plk1, ROCK II, Map4, VAMP8, Cep55, SEPT2, SEPT7, and SEPT11 at the midbody is not perturbed upon SEPT9 depletion. Video 1 shows the division of HeLa cells treated with control siRNA. Videos 2 and 3 show the division of HeLa cells upon depletion of SEPT2 and SEPT11, respectively. Videos 4 and 5 show the division of a HeLa cell upon depletion of SEPT9. Video 4 shows that cleavage furrow contraction is not affected by SEPT9 depletion, whereas Video 5 demonstrates that SEPT9 depletion impairs midbody abscission. Online supplemental material is available at http://www.jcb.org/cgi/content/full/jcb.201006031/DC1.

We thank all members of the Trimble and Kahr laboratories, M. Woodside and P. Paroutis for input and assistance, and Dr. C. Tailor, Dr. S. Duffy, Dr. B. Zieger, Dr. T. Weimbs, Dr. K. Kutsche, and Dr. E. Petty for reagents.

This work was supported by the Canadian Cancer Society. M.P. Estey is the recipient of a Canada Graduate Scholarship from the Natural Sciences and Engineering Research Council of Canada, C. Di Ciano-Oliveira is supported by a postdoctoral fellowship from the Ontario Ministry of Research and Innovation, and W.S. Trimble holds a Canada Research Chair in Molecular Cell Biology.

Submitted: 4 June 2010
Accepted: 11 October 2010

References

Beites, C.L., H. Xie, R. Bowser, and W.S. Trimble. 1999. The septin CDCrel-1 binds syntaxin and inhibits exocytosis. *Nat. Neurosci.* 2:434–439. doi:10.1038/8100

Burrows, J.F., S. Chanduloy, M.A. McIlhatton, H. Nagar, K. Yeates, P. Donaghy, J. Price, A.K. Godwin, P.G. Johnston, and S.E. Russell. 2003. Altered expression of the septin gene, SEPT9, in ovarian neoplasia. *J. Pathol.* 201:581–588. doi:10.1002/path.1484

Di Ciano-Oliveira, C., M. Lodyga, L. Fan, K. Szászi, H. Hosoya, O.D. Rotstein, and A. Kapus. 2005. Is myosin light-chain phosphorylation a regulatory signal for the osmotic activation of the Na+-K+-2Cl- cotransporter? *Am. J. Physiol. Cell Physiol.* 289:C68–C81. doi:10.1152/ajpcell.00631.2004

Dobbelaere, J., and Y. Barral. 2004. Spatial coordination of cytokinetic events by compartmentalization of the cell cortex. *Science.* 305:393–396. doi:10.1126/science.1099892

Dunn, K.C., A.E. Aotaki-Keen, F.R. Putkey, and L.M. Hjelmeland. 1996. ARPE-19, a human retinal pigment epithelial cell line with differentiated properties. *Exp. Eye Res.* 62:155–169. doi:10.1006/exer.1996.0020

Eggert, U.S., T.J. Mitchison, and C.M. Field. 2006. Animal cytokinesis: from parts list to mechanisms. *Annu. Rev. Biochem.* 75:543–566. doi:10.1146/annurev.biochem.74.082803.133425

Friedrich, G.A., J.D. Hildebrand, and P. Soriano. 1997. The secretory protein Sec8 is required for paraxial mesoderm formation in the mouse. *Dev. Biol.* 192:364–374. doi:10.1006/dbio.1997.8727

Fujiwara, T., M. Bandi, M. Nitta, E.V. Ivanova, R.T. Bronson, and D. Pellman. 2005. Cytokinesis failure generating tetraploids promotes tumorigenesis in p53-null cells. *Nature.* 437:1043–1047. doi:10.1038/nature04217

Glotzer, M. 2001. Animal cell cytokinesis. *Annu. Rev. Cell Dev. Biol.* 17:351–386. doi:10.1146/annurev.cellbio.17.1.351

Gonzalez, M.E., E.A. Peterson, L.M. Privette, J.L. Loffreda-Wren, L.M. Kalikin, and E.M. Petty. 2007. High SEPT9_v1 expression in human breast cancer cells is associated with oncogenic phenotypes. *Cancer Res.* 67:8554–8564. doi:10.1158/0008-5472.CAN-07-1474

Goodall, H., and M.H. Johnson. 1984. The nature of intercellular coupling within the preimplantation mouse embryo. *J. Embryol. Exp. Morphol.* 79:53–76.

Gromley, A., C. Yeaman, J. Rosa, S. Redick, C.T. Chen, S. Mirabelle, M. Guha, J. Sillibourne, and S.J. Doxsey. 2005. Centriolin anchoring of exocyst and SNARE complexes at the midbody is required for secretory-vesicle-mediated abscission. *Cell.* 123:75–87. doi:10.1016/j.cell.2005.07.027

Hall, P.A., and S.E. Russell. 2004. The pathobiology of the septin gene family. *J. Pathol.* 204:489–505. doi:10.1002/path.1654

Hall, P.A., E. Bruford, S.E.H. Russell, I.G. Macara, and J.R. Pringle. 2008a. Mammalian septin nomenclature. *In* The Septins. P.A. Hall, S.E.H. Russell, and J.R. Pringle, editors. Wiley-Blackwell, West Sussex, England, UK. 351–354.

Hall, P.A., S.E.H. Russell, and J.R. Pringle, editors. 2008b. The Septins. Wiley-Blackwell, West Sussex, England, UK. 370 pp.

Huang, Y.W., M. Yan, R.F. Collins, J.E. Diciccio, S. Grinstein, and W.S. Trimble. 2008. Mammalian septins are required for phagosome formation. *Mol. Biol. Cell.* 19:1717–1726. doi:10.1091/mbc.E07-07-0641

Ihara, M., A. Kinoshita, S. Yamada, H. Tanaka, A. Tanigaki, A. Kitano, M. Goto, K. Okubo, H. Nishiyama, O. Ogawa, et al. 2005. Cortical organization by the septin cytoskeleton is essential for structural and mechanical integrity

of mammalian spermatozoa. *Dev. Cell.* 8:343–352. doi:10.1016/j.devcel.2004.12.005

Joo, E., M.C. Surka, and W.S. Trimble. 2007. Mammalian SEPT2 is required for scaffolding nonmuscle myosin II and its kinases. *Dev. Cell.* 13:677–690. doi:10.1016/j.devcel.2007.09.001

Kinoshita, M. 2008. Insight into septin functions from mouse models. *In* The Septins. P.A. Hall, S.E.H. Russell, and J.R. Pringle, editors. Wiley-Blackwell, West Sussex, England, UK. 319–336.

Kinoshita, M., S. Kumar, A. Mizoguchi, C. Ide, A. Kinoshita, T. Haraguchi, Y. Hiraoka, and M. Noda. 1997. Nedd5, a mammalian septin, is a novel cytoskeletal component interacting with actin-based structures. *Genes Dev.* 11:1535–1547. doi:10.1101/gad.11.12.1535

Kinoshita, M., C.M. Field, M.L. Coughlin, A.F. Straight, and T.J. Mitchison. 2002. Self- and actin-templated assembly of Mammalian septins. *Dev. Cell.* 3:791–802. doi:10.1016/S1534-5807(02)00366-0

Kissel, H., M.M. Georgescu, S. Larisch, K. Manova, G.R. Hunnicutt, and H. Steller. 2005. The Sept4 septin locus is required for sperm terminal differentiation in mice. *Dev. Cell.* 8:353–364. doi:10.1016/j.devcel.2005.01.021

Kremer, B.E., T. Haystead, and I.G. Macara. 2005. Mammalian septins regulate microtubule stability through interaction with the microtubule-binding protein MAP4. *Mol. Biol. Cell.* 16:4648–4659. doi:10.1091/mbc.E05-03-0267

Low, C., and I.G. Macara. 2006. Structural analysis of septin 2, 6, and 7 complexes. *J. Biol. Chem.* 281:30697–30706. doi:10.1074/jbc.M605179200

Low, S.H., X. Li, M. Miura, N. Kudo, B. Quiñones, and T. Weimbs. 2003. Syntaxin 2 and endobrevin are required for the terminal step of cytokinesis in mammalian cells. *Dev. Cell.* 4:753–759. doi:10.1016/S1534-5807(03)00122-9

Lowery, D.M., K.R. Clauser, M. Hjerrild, D. Lim, J. Alexander, K. Kishi, S.E. Ong, S. Gammeltoft, S.A. Carr, and M.B. Yaffe. 2007. Proteomic screen defines the Polo-box domain interactome and identifies Rock2 as a Plk1 substrate. *EMBO J.* 26:2262–2273. doi:10.1038/sj.emboj.7601683

Montagna, C., M.S. Lyu, K. Hunter, L. Lukes, W. Lowther, T. Reppert, B. Hissong, Z. Weaver, and T. Ried. 2003. The Septin 9 (MSF) gene is amplified and overexpressed in mouse mammary gland adenocarcinomas and human breast cancer cell lines. *Cancer Res.* 63:2179–2187.

Nagata, K., A. Kawajiri, S. Matsui, M. Takagishi, T. Shiromizu, N. Saitoh, I. Izawa, T. Kiyono, T.J. Itoh, H. Hotani, and M. Inagaki. 2003. Filament formation of MSF-A, a mammalian septin, in human mammary epithelial cells depends on interactions with microtubules. *J. Biol. Chem.* 278:18538–18543. doi:10.1074/jbc.M205246200

Osaka, M., J.D. Rowley, and N.J. Zeleznik-Le. 1999. MSF (MLL septin-like fusion), a fusion partner gene of MLL, in a therapy-related acute myeloid leukemia with a t(11;17)(q23;q25). *Proc. Natl. Acad. Sci. USA.* 96:6428–6433. doi:10.1073/pnas.96.11.6428

Petronczki, M., M. Glotzer, N. Kraut, and J.M. Peters. 2007. Polo-like kinase 1 triggers the initiation of cytokinesis in human cells by promoting recruitment of the RhoGEF Ect2 to the central spindle. *Dev. Cell.* 12:713–725. doi:10.1016/j.devcel.2007.03.013

Russell, S.E., M.A. McIlhatton, J.F. Burrows, P.G. Donaghy, S. Chanduloy, E.M. Petty, L.M. Kalikin, S.W. Church, S. McIlroy, D.P. Harkin, et al. 2000. Isolation and mapping of a human septin gene to a region on chromosome 17q, commonly deleted in sporadic epithelial ovarian tumors. *Cancer Res.* 60:4729–4734.

Scott, M., P.L. Hyland, G. McGregor, K.J. Hillan, S.E. Russell, and P.A. Hall. 2005. Multimodality expression profiling shows SEPT9 to be overexpressed in a wide range of human tumours. *Oncogene.* 24:4688–4700. doi:10.1038/sj.onc.1208574

Scott, M., W.G. McCluggage, K.J. Hillan, P.A. Hall, and S.E. Russell. 2006. Altered patterns of transcription of the septin gene, SEPT9, in ovarian tumorigenesis. *Int. J. Cancer.* 118:1325–1329. doi:10.1002/ijc.21486

Sirajuddin, M., M. Farkasovsky, F. Hauer, D. Kühlmann, I.G. Macara, M. Weyand, H. Stark, and A. Wittinghofer. 2007. Structural insight into filament formation by mammalian septins. *Nature.* 449:311–315. doi:10.1038/nature06052

Spiliotis, E.T., M. Kinoshita, and W.J. Nelson. 2005. A mitotic septin scaffold required for Mammalian chromosome congression and segregation. *Science.* 307:1781–1785. doi:10.1126/science.1106823

Steigemann, P., and D.W. Gerlich. 2009. Cytokinetic abscission: cellular dynamics at the midbody. *Trends Cell Biol.* 19:606–616. doi:10.1016/j.tcb.2009.07.008

Straight, A.F., C.M. Field, and T.J. Mitchison. 2005. Anillin binds nonmuscle myosin II and regulates the contractile ring. *Mol. Biol. Cell.* 16:193–201. doi:10.1091/mbc.E04-08-0758

Surka, M.C., C.W. Tsang, and W.S. Trimble. 2002. The mammalian septin MSF localizes with microtubules and is required for completion of cytokinesis. *Mol. Biol. Cell.* 13:3532–3545. doi:10.1091/mbc.E02-01-0042

Tada, T., A. Simonetta, M. Batterton, M. Kinoshita, D. Edbauer, and M. Sheng. 2007. Role of Septin cytoskeleton in spine morphogenesis and dendrite development in neurons. *Curr. Biol.* 17:1752–1758. doi:10.1016/j.cub.2007.09.039

Tooley, A.J., J. Gilden, J. Jacobelli, P. Beemiller, W.S. Trimble, M. Kinoshita, and M.F. Krummel. 2009. Amoeboid T lymphocytes require the septin cytoskeleton for cortical integrity and persistent motility. *Nat. Cell Biol.* 11:17–26. doi:10.1038/ncb1808

Weirich, C.S., J.P. Erzberger, and Y. Barral. 2008. The septin family of GTPases: architecture and dynamics. *Nat. Rev. Mol. Cell Biol.* 9:478–489. doi:10.1038/nrm2407

Xie, H., M. Surka, J. Howard, and W.S. Trimble. 1999. Characterization of the mammalian septin H5: distinct patterns of cytoskeletal and membrane association from other septin proteins. *Cell Motil. Cytoskeleton.* 43:52–62. doi:10.1002/(SICI)1097-0169(1999)43:1<52::AID-CM6>3.0.CO;2-5

Xie, Y., J.P. Vessey, A. Konecna, R. Dahm, P. Macchi, and M.A. Kiebler. 2007. The GTP-binding protein Septin 7 is critical for dendrite branching and dendritic-spine morphology. *Curr. Biol.* 17:1746–1751. doi:10.1016/j.cub.2007.08.042

Yamamoto, K., F. Shibata, M. Yamaguchi, and O. Miura. 2002. Fusion of MLL and MSF in adult de novo acute myelomonocytic leukemia (M4) with t(11;17)(q23;q25). *Int. J. Hematol.* 75:503–507. doi:10.1007/BF02982114

Zhao, W.M., A. Seki, and G. Fang. 2006. Cep55, a microtubule-bundling protein, associates with centralspindlin to control the midbody integrity and cell abscission during cytokinesis. *Mol. Biol. Cell.* 17:3881–3896. doi:10.1091/mbc.E06-01-0015

Zhu, M., F. Wang, F. Yan, P.Y. Yao, J. Du, X. Gao, X. Wang, Q. Wu, T. Ward, J. Li, et al. 2008. Septin 7 interacts with centromere-associated protein E and is required for its kinetochore localization. *J. Biol. Chem.* 283:18916–18925. doi:10.1074/jbc.M710591200